STRUCTURE AS WELL AS PHOTOLUMINESCENCE DE-CONVOLUTION OF ZnO MESOPOROUS SYNTHESIZED BY SIMPLE SOL-GEL METHOD

A. MODWI[a,c*], M. A. ABBO[b,c], E. A. HASSAN[c], A. HOUAS [a, d]
[a]*Al Imam Mohammad Ibn Saud Islamic University (IMSIU), College of Sciences, Department of Chemistry, Riyadh 11623, Saudi Arabia.*
[b]*Taif University, College of Education and Science, Chemistry Department, Saudi Arabia.*
[c]*Sudan University of Science and Technology, College of Science, Chemistry Department, , Khartoum, Sudan.*
[d]*Unité de Recherche Catalyse et Matériaux pour l'Environnement et les Procédés (URCMEP); Université de Gabès; Campus Universitaire -Cité Erriadh-6072 Gabès, Tunisie*

Herein ZnO nanoparticles has been successfully synthesized via a simple and fast sol gel method. The prepared nanomaterials were annealed then characterized using XRD, BET, SEM, EDX, TGA, DTG and PL. The results revealed the formation of wurtzite ZnO nanoparticles with surface area that decreased from 109.7 to7.48 m^2/g and a corresponding 16.03 to 25.03 nm mean diameter due to the rise in annealing temperature. The BET isotherms analysis indicated mesoporous nanoparticles supporting the data obtained by particle size. The TGA and DTG results indicated the formation of zinc oxide nanoparticles. The PL study showedUV bands emissions intensity increased from 7.28 to 67.8 % as the annealing temperature rise from 250 to 550 ^oC respectively.

(Received March 26, 2016; Accepted July 15, 2016)

Keywords: ZnO, Sol-gel, Annealing, XRD and Photoluminescence de-convolution

1. Introduction

Nanomaterials have attracted tremendous interest due to their noticeable performance in electronics, optics, and photonics. Due to its properties, such as semiconducting, optical, mechanical properties, antibacterial and catalytic activity, zinc oxide is widely applied in the field of optoelectronics, photocatalysis, pharmaceuticals, textiles and cosmetics [1-5]. ZnO is a semiconductor material with direct wide band gap energy (3.37 eV) and a large exciton binding energy (60meV) at room temperature [6]. Different synthetic methods have been employed to prepare ZnO nanoparticles such as sol–gel [7], precipitation [8], co-precipitation [9], hydrothermal [10] spray pyrolysis [11], microwave irradiation [12], chemical vapor deposition [13], pulsed laser deposition [14]The most important and more common method to prepare nanoparticles is the sol-gel method, because of its simple and low cost [15]. In the sol-gel method, many preparation parameters may influence the properties of the final prepared nanomaterial: the nature of precursors, the solvents used the pH and specifically the nature of the catalysts used during the preparation and the annealing temperature and duration. Among all of these parameters, we looked at the last two, using to our knowledge the 2.3-dihydroxysuccinic acid for the first time as a catalyst in the sol-gel method and studying the effect of annealing temperature.

Thus, in this study, ZnO nanoparticles have been prepared by using 2.3-dihydroxysuccinic acid as a catalyst. The obtained products were annealed 250, 350, 450 and 550 °C. The effect of annealing temperature on the structure, the morphology, the surface area, the thermal stability and the spectral properties was studied extensively.

* Corresponding author: abuelizkh81@gmail.com

2. Experimental

2.1 Preparation of ZnO nanoparticles

Zinc acetate dihydrate ($Zn(CH_3COO)_2.2H_2O$), absolute methanol 99.99%, 2,3.dihydroxysuccinic acid $(CHOH\text{-}COOH)_2$ were purchased from Panreac and all chemicals were utilized without further purification. As described in our previous work [16], a certain amount of zinc acetate was dissolved in a 75 mL of methanol and stirred at 400 rpm for 30 minutes. The 2.3-dihydroxysuccinic acid catalyst was dissolved in approximately 45mL of distilled water and stirred for 30 minutes. The solution of 2.3-dihydroxysuccinic acid was added dropwise to the mixture. Under vigorous magnetic agitation a white gel was rapidly formed at room temperature and then oven dried at 110 °C for16 hours. The obtained powder was grinded prior to annealing in a tubular furnace at different temperatures ranging from 250 to 550 °C for an hour. The outline shown in (Figure. 1) summarizes the synthesis steps.

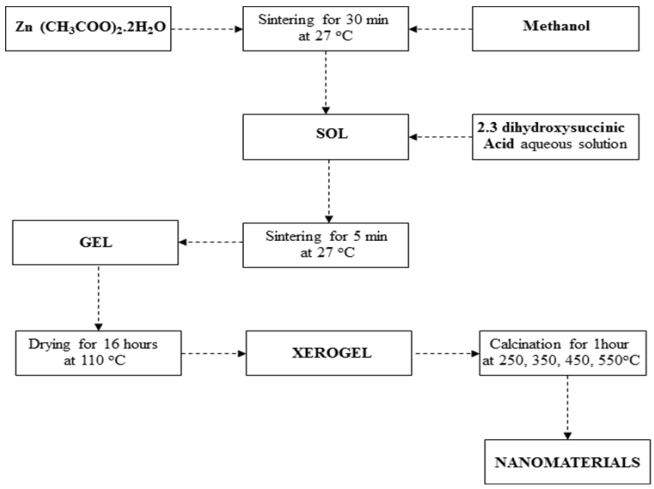

Fig.1. Outline of the procedure for synthesis of ZnO nanomaterials

2.2 Characterization of ZnO

The structure, crystallinity and average particles size of photocatalysts were determined by the powder X-ray diffraction patterns, the samples were recorded by a diffractometer (D8 Advance Bruker) using Cu-Kα radiation, λ = 0.15406 nm, accelerating voltage is 40 kV and 20 -80° as scanning angle. The surface area and porosity of photocatalysts were determined using a Micrometrics ASAP 2020 apparatus, (Degas temperature: ambient to 200°C for 20 minutes with pressure range from 0 to 950 mmHg). The morphology of the nanopowder samples was examined by a scanning electron microscope. The samples were previously oven dried at 105°C and coated with a thin film of gold to provide ZnO powder surface with electrical conduction. The thermal decomposition behaviors of samples were evaluated using Thermogravimetric (Model: Mettler Toledo). The sample was heated from room temperature to 1100 °C in a crucible volume up to 150 µL with heating rate from 0.02 to 250K/min. For the photoluminescence characterization, a Perkin Elmer LS45 luminescence (PL) was used. The excitation source is a special Xenon flash tube producing an intense short duration pulse of radiation over the spectral range with a excitation wavelength at 325 nm.

3. Results and discussion

3.1 X-ray diffraction of ZnO nanoparticles

Figure (2) depicts the XRD patterns for the prepared ZnO nanoparticles. The characteristic broad peaks at position (31.61, 34.39 , 36.11, 47.40, 56.52, 62.72, 66.29, 67.91 and 69.08 deg.) are clearly shown. These data are inconsistence with standard card (JCPDS 36-1451) file for ZnO

indicating hexagonal wurtzite structure emphasizing the formation of well-crystallized ZnO nanoparticles. After annealing, the intensity of the XRD peaks has been altered.This change is clearly manifested by the increase of the principal peak (101) intensity, its shift and the narrowing of its shape. This observation reveals an increase of the crystallite size [17]. The average crystalline size (D) of the prepared nanomaterialpresented in (Table.1) was calculated using the well know Scherrer's equation:

$$D = \frac{0.9\lambda}{\beta \cos\theta} \qquad (1)$$

Where λ is the wavelength of Cu Kα radiation, β is full width half maxima (FWHM) of the diffraction peak and Θ is the Bragg peak angle. As a result of annealing at different temperatures, the average crystallite size of ZnO was found to increase from 16.12 to 25.03 nm with the rise in temperature from 250 to 550°C respectively.

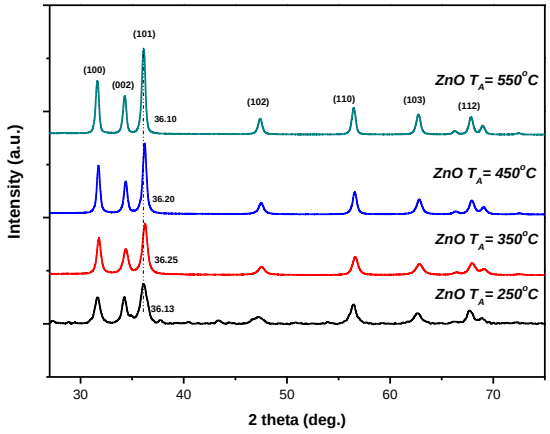

Fig.2. XRD patterns of ZnO at 250, 350, 450 and 550 °C

3.2 Surface area analysis

To further confirm the porous structure of the annealed ZnO nanoparticles, N_2 adsorption-desorption isotherms and the derived pore-size distribution have been determined. As shown in Figure.3.the samples display a Type IV isotherm [18] corresponding to a capillary condensation according to IUPAC classification.The isotherms show a hysteresis loop of Type H_3 characteristics of a mesoporous material, which did not exhibit limiting adsorption at high relative pressure (≈1) suggesting a slit-shaped pores. All desorption branches are different from adsorption ones indicating differences in their pore's texture [19]. Barret-Joyner-Halenda (BJH) average pore diameter [20]for all nanoparticles is depicted in (Figure.3.). All plots are centered in the mesopores range confirming the Type IV adsorption isotherm. BJH pore size distribution of nonmaterial annealed at T_A= 250°C (inset) with an average pore diameter centered at around 9 nm shows features different from that of ZnO annealed at higher temperatures T_A= 350, 450 and 550°C. This is an indication of a modification in pore texture. In the light of these observations, we can notice a significant effect of the annealing temperature on the both specific surface area and the pore size distribution of the ZnO photocatalysts (Table.1). Discernible, the increase of the annealing temperature, we notice a remarkable decrease in the surface area from 109.7 to 7.48 m^2/g when T_A increases from 250 to 550°C together with an increase in the average size distribution (Figure.4.). These phenomena can be correlated to a pores clogging caused by possible aggregation occurring as the annealing temperature increases as per the Oswald ripening [21].

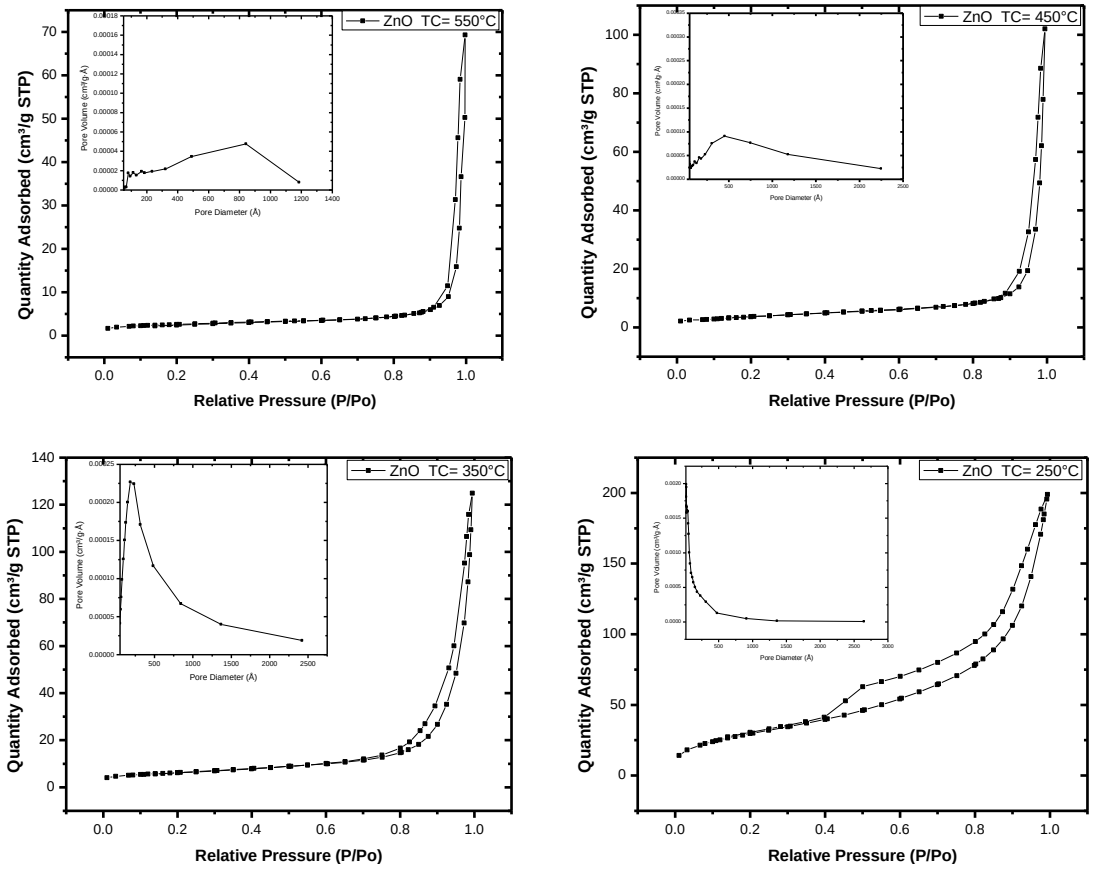

Fig..3. Nitrogen adsorption-desorption isotherms on ZnO nanoparticles annealed at different temperatures and inset Barret-Joyner-Halenda (BJH) pore size distribution

Table (1): Crystallite size, BET surface area and average pore diameter of ZnO nanoparticles

ZnO annealing temperature (°C)	Crystallite size (nm) from XRD	BET Surface area (m^2/g)	Average pore diameter (nm)
250	16.12	109.7	9.96
350	18.17	22.13	33.53
450	24.26	13.21	39.8
550	25.03	7.48	44.03

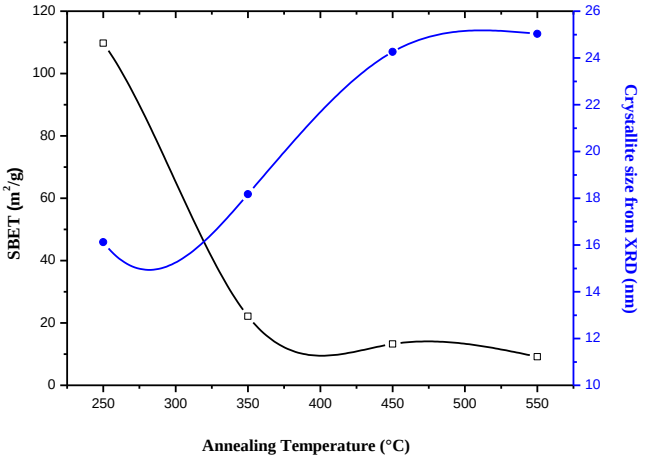

Fig.4.Effect of annealing temperature on the S_{BET} and the crystallite size

3.3 Thermogravimetric analysis

The thermal stability of precursor of ZnO prepared by the sol-gel method was studied by TGA and DTG in the temperature range of 0 to 700 °C as presented in (Figure.5.) The weight loss of the xerogel occurs in three steps. The first step of (8%) weight loss is in the range from 100°C to 180°C, due to the dehydration of surface absorbed water [22].The second step weight loss (17 %) takes place in the range from 180 to 300°C corresponding to the elimination of dihydrate from zinc acetate and the solvent methanol remains. The third stage of weight loss (41.5 %) may be attributed decomposed of zinc2.3-dihydroxysuccinate to form the ZnO nanoparticles. On the other hand, the DTA curve shows two prominent endothermic peaks at 244 °C to 354°Cindicating the two main processes of dehydration and organics decomposition [23].

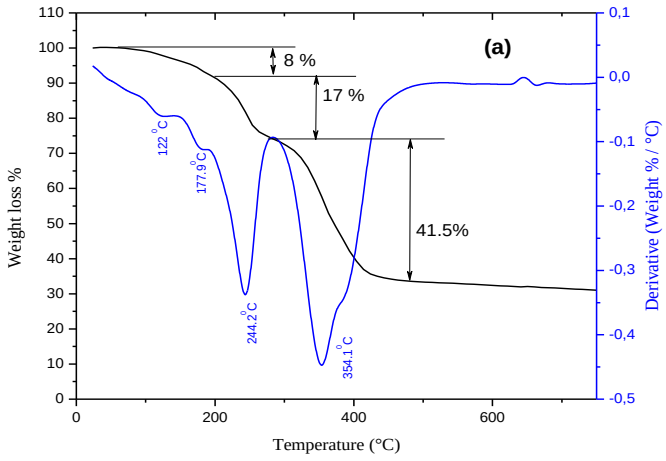

Fig.5. TGA and DTG curves of ZnO xerogel pure

3.4 SEM and EDX of ZnO annealed at 550°C

Fig.6 illustrates the SEM micrograph obtained for ZnO annealed at 550 °C. The obtained powder is spherical in shape due to the annealing temperature effect [24]. Further, the EDX image captured shows prominent peaks that confirm the existence of Zn and O in the sample with the ratio 83.47 to 16.53 % respectively. This finding indicates the purity of nanoparticles formed as well as it supports the XRD results.

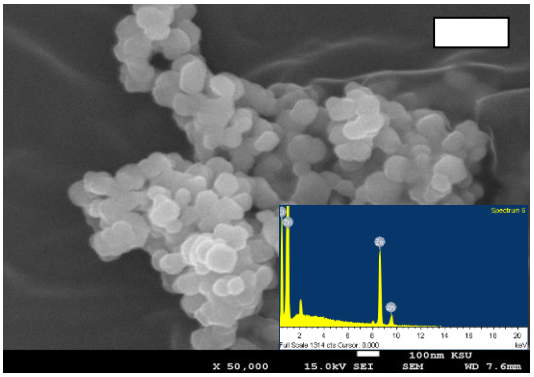

Fig.6. SEM and EDAX of ZnO annealed at 550 °C

3.5 Photoluminescence (PL) of ZnO nanomaterials

Photoluminescence (PL) spectra of ZnO nanoparticles were determined, to explore the effect of the annealing temperature on its optical properties. Fig.7 shows the emission spectrum of ZnO specimens using an excitation wavelength of 325 nm at room temperature. The (PL) emission is observed for all the samples (T_A = 250 to 550 °C) covering the range from a short wavelength of 325nm to a long wavelength of 550nm.All the PL spectra of the obtained samples show one intrinsic UV emission band in the range of 385 to 357nm, which seems to belong to the exciton recombination related to near band edge emission (NEB). Furthermore, the intensity of the PL peak in the UV region increasesfrom 7.28 to 67.8 % as the annealing temperature rises from 250 to 550 ^{o}C. This finding demonstrates the enhancement in the crystalline nature of the specimens [25]. For more understanding, the bands can be well de-convoluted using a Gussian fitting ($R^2 > 0.99$) to three bands: in the range 317 -418 nm (Figure.8). The UV bands emissions are more dominant than the visible band emissions. In a similar study the PL bands were de-convoluted into four bands centered at 388, 414, 466 and 573nm [26]. The PL spectrum of ZnO annealed at 250°C shows UV Near-Band-Edge (NBE) of 317-355 nm and a small shoulder of green emission band at ≈450 nm (Figure.8.(D)). However, this latest visible band disappears whenthe annealing temperature increases. In a previous work Manzano et al. [34] reported that green emission was due to -OH defects which reduce at annealing temperature higher than 250°C. From figure. 8(A), (B), (C) and (D) and table .2, one can observe the variations of the positions and the intensities of the PL UV and visible bands. The UV bands known as excitonic mission are resulting from the excitation of electrons from the valence to this level in the band gap. Afterwards, they emitthe same amount of energy, relax backto the valence bandandget associatedwithaholetoforma pairof exciton [27]. As the temperature was increased, the intensities of the UV bands shifted to longer wavelength as well as being enhanced (Figure.8 and Table.2). The change of PL bands due to annealing temperature influence was previously observed [28]. Omari et al. [17] reported a shift in the UV bands from 371 to 386 nm when a sample of ZnO was heated from room temperature to 500 °C.A band in the blue-violet emission at 400-420 nm is exhibited by all the samples (Figure.8 and Table.2). The visible emission (blue-violet 400-420 nm) may belinked to a very fast trapping of the photo-generated hole at the particle surface, which then tunnels into the bulk of the nanoparticles to an oxygen vacancy. Thus, a center is created and gets combined with a shallowly trapped electron to give the trap emission [29]. Zeng et al. [30] assigned the PL blue emission to the $Zn_i \rightarrow V_B$ transition, where they identified Zn_i as deeper levels lying about 0.37 eV below the C_B. Meanwhile Wu et al. [31] attributed it to the $C_B \rightarrow O_i$ transition. This blue/violet band has been also reported bysome researchers [32,33].

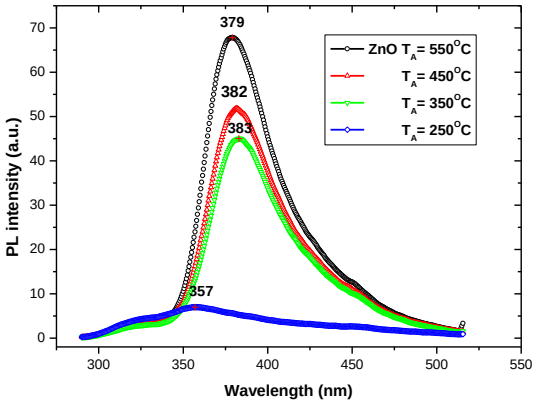

Fig.7. PL spectra of the pure ZnO annealed at different temperatures (from T_A= 250 to 550 ^oC), at wavelength 325nm excitation

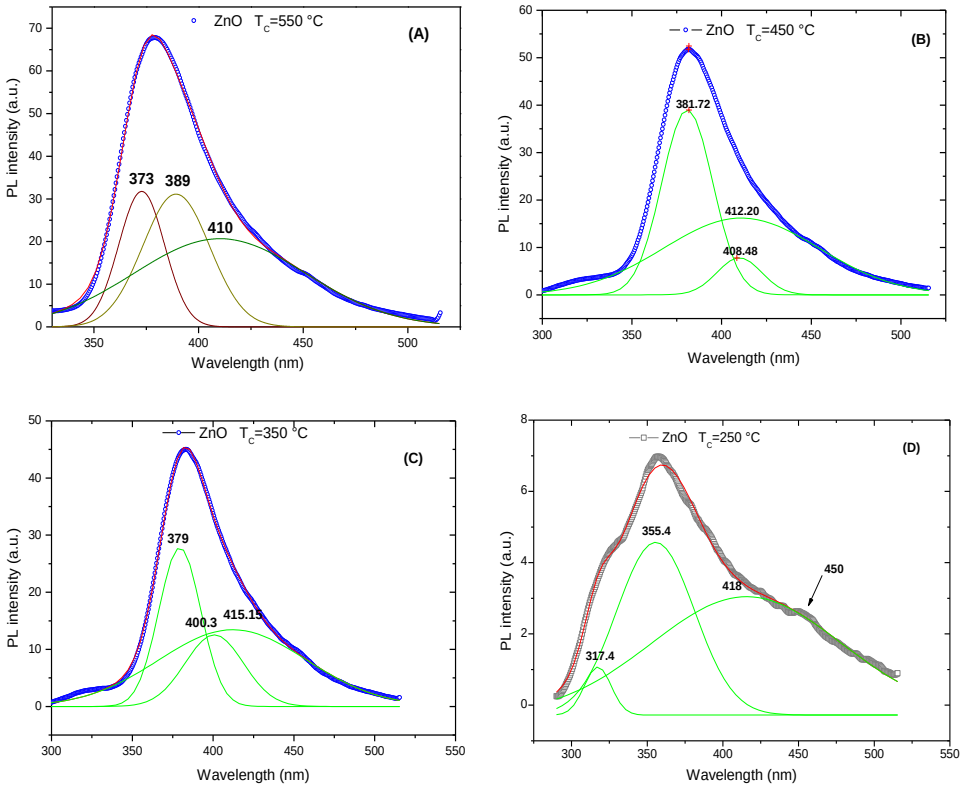

Fig..8. PL emissions spectra of pure ZnO annealed at (A) T_A =550°C, (B) T_A=450°C, (C) T_A=350°C, (D) T_A=250°C using the excitation wavelength at 325 nm.

Table.2. Photoluminescence Emission Values of pure ZnO annealed at various temperatures deduced from deconvolution by Gaussian function of PL spectra:

ZnO annealing temperature(°C)	NEB (nm)	NEB intensity (a.u)	Blue emission (nm)	R^2%
550	373- 389	32.40- 31.41	410 (violet)	99.86
450	381	39.03	408 - 412	99.86
350	379	27.81	400 - 415	99.90
250	317 - 355	1.37- 4.91	418	99.65

4. Conclusions

In this study, ZnO nanoparticles were prepared by simple sol-gel method using 2.3-dihydroxysuccinic acid as gelling agent. The produced gel was dried at 110 °C and annealing at different temperature 250, 350, 450 and 550 °C and then characterized by XRD, BET, TGA, SEM, EDX and PL. The XRD and SEM analysis indicate the formation of a mesoporous ZnO nanoparticles. The study reveals the formation of mesoporous nanoparticles with sizes increasingand a concurrent decreasing in the surface area with the annealing temperature rise.One major PL peak in the UV region, with an intensity from 7.28 to 67.8 % according to the annealing temperature, was observed. This intensity increasing induces an enhancement in the crystalline nature of the nanoparticles. PL spectrade-convolutionshowsa peak in UV region and two peaks in visible emission with variable positions and intensities according to the annealing temperature.

References

[1] A. Kołodziejczak-Radzimska and Jesionowski T., Materials, **7**, 2833(2014)

[2] M.Mehedi Hassan, A. S. Ahmed, M. Chaman, W.Khan, a. H. Naqvi, A. Azam, Materials Research Bulletin, **47**(12), 3952 (2012).

[3] A.Iribarren, E., Hernández-rodríguez, L. Maqueira, Materials Research Bulletin, n **60**, 376 (2014).

[4] A. K., Mishra, D. Das, Materials Science & Engineering B, **171**(1-3), 5 (2010).

[5] R., Saleh, N. F. Djaja, SUPERLATTICES AND MICROSTRUCTURES, **74**, 217 (2014).

[6] F. Lu,W.Cai,Y.Zhang, Advanced FunctionalMaterials, **18**(7), 1047 (2008).

[7] J. Yang, L. Feia, H. Liua, Y. Liu, M. Gaoa, Y. Zhanga, L. Yanga, J. Alloys Compd. **509,**3672 (2011).

[8] Y. Yang, H. Chen, B. Zhao, X. Bao, J. Cryst. Growth **263**,447 (2004).

[9] R. Chauhan, A. Kumar, R.P. Chaudharya, J. Chem. Pharm. Res. **2**(4),178 (2010).

[10] R. Savu, R. Parra, E. Joanni, B. Jancar, S.A. Elizario, R. de Camargo, P.R. Bueno, J.A. Varela, E. Longo, M.A. Zaghate, J. Cryst. Growth **311,**4102 (2009).

[11] Y. Ni, X. Cao, G. Wu, G. Hu, Z. Yang, X. Wei, Nanotechnology **18,**155603 (2007).

[12] C.R. Shabnam, P. Arun Kant, J. Lumin. **132**,1744 (2012).

[13] T.H. Vlasenflin, M. Tanaka, Solid State Commun. **142**,292 (2007).

[14] Y. Adachi, N. Ohashi, T. Ohnishi, T. Ohgaki, I. Sakaguchi, H. Haneda, M. Lippmaa, J. Mater. Res. **23**,3269 (2008).

[15] J. Lee, A. J.Easteal, U. Pal, D.Bhattacharyya, Current Applied Physics, **9**,792 (2009).

[16] A. Modwi, M. A. Abbo, E. A. Hassan, K. K.Taha, L.Khezami, A. Houas, Journal of Ovonic research. **12**(2), 59(2016).

[17] K. Omri, I. Najeh, R. Dhahri, J. El Ghoul, L. El Mir. Microelectronic Engineering **128,**53 (2014).

[18] F Rouquerol, J Rouquerol, Sing K. Adsorption by powders and porous solids. London: Academic Press; 1999.

[19] M.Z.; Hussein, S.H.; Al Ali, Z.; Zainal, M.N. Hakim, Int. J. Nanomed., **6**, 1373(2011)

[20] EP Barrett, LG Joyner, PP Halenda. J Am ChemSoc;**73**, 373(1951)

[21] P. Singh, A. Kumar, D. Deepak and D. Kaur.Optical Materials **30**,1316 (2008).

[22] D. Rauofi. Renewable Energy, **50,**932 (2013).

[23] J. Zhou, F. Zhao, Y. Wang, Y. Zhang and L. Yang. Journal of Luminescence, **122-123,**195 (2007).

[24] R. Y.Hong, J. Z. Qian,J. X. Powder Technol., **163**,160 (2006).

[25] MA Gondal, QA Drmosh, ZH Yamani, TA Saleh. Appl Surf Sci;**256**, 298(2009)

[26] G.Patwari, B.J.Bodo, R. Singha,P.K. KalitaResearch Journal of Chemical Sciences **3**(9), 45 (2013).

[27] D, Behera, B. S. Acharya. J. Lumin. **128**,1577 (2008).

[28] N.Tu, N.T.Tuan, N. V. Dung, N.D.Cuong, N.D.T.Kien, P.T.Huy, N.V. Hieu D.H.Nguyen. Journal ofLuminescence**156**, 199 (2014).

[29] A. van Dijken, E.A. Meulenkamp, D. Vanmaekelbergh, A. Meijerink, J. Lumin. **87,**454(2000).
[30] HZeng, GDuan, YLi, SYang, XXu, WCai,:AdvFunct Mater, **20**, 5612010
[31] XLWu, GGSiu, CLFu, HCOng: Appl Phys Lett, **78**, 2285(2001)
[32] J. Xu, J. Zhang, W. Ding, W. Yang, G. Cheng, Y. Du, J. Zuo, C. Xu, Y. Zhang, Z. Du,. Solid State Commun.**101**,467 (1997).
[33] T.V. Butkhuzi, A.V. Bureyev, A.N. Geogobian, N.P. Kekelidze, T.G. Khulordava. J. Cryst. Growth **117**,366 (1992) -369.
[34] C. V.Manzano, D.Alegre O., Caballero-Calero, B. Alen, Martin-Gonzalez. J. Appl. Phys. **110**(4), 04538 (2011).